Chemical Physics 357 (2009) 163–170

Contents lists available at ScienceDirect

Chemical Physics

journal homepage: www.elsevier.com/locate/chemphys

Trapping kinetics in isolated cyanobacterial PS I complexes

Chavdar Slavov [a], Eithar El-Mohsnawy [b,1], Matthias Rögner [b], Alfred R. Holzwarth [a,*]

[a] Max-Planck-Institut für Bioanorganische Chemie, Stiftstr. 34-36, D-45470 Mülheim a.d. Ruhr, Germany
[b] Lehrstuhl Biochemie der Pflanzen, Ruhr-Universität Bochum, Universitätsstrasse 150, D-44801 Bochum, Germany

ARTICLE INFO

Article history:
Received 11 August 2008
Accepted 22 December 2008
Available online 27 December 2008

Keywords:
Photosynthesis
Photosystem I
'Red' chlorophylls
Trapping kinetics
Charge separation

ABSTRACT

The excitation energy trapping and the role of the 'red' chlorophyll (Chl) states in the photosystem (PS) I monomers and trimers from the cyanobacterium *Thermosynechococcus elongatus* were studied. We demonstrate the adequacy of the "charge recombination" model for the trapping kinetics. On the basis of this model the reaction center excited state can be resolved. The overall kinetics is shown to be trap-limited even though the presence of the 'red' Chls induces a substantial slowing down (~60%) of the trapping. Two kinetically different 'red' Chl pools were resolved. Both of these 'red' pools originate from the same groups of pigments in either of the two aggregation states. This indicates that careful isolation does not disturb substantially the 'red' Chls and we can exclude their location at the monomer–monomer interface. Acceleration of the secondary electron transfer step in the studied complexes as compared to PS I from mesophilic organisms is observed.

1. Introduction

Photosystem I (PS I) is one of the largest membrane complexes, hosting 127 co-factors [1]. It is involved, together with PS II, in conducting the light reactions of photosynthesis. The structure of the cyanobacterial PS I complex is resolved to 2.5 Å resolution [1]. It seems, that naturally most of the cyanobacterial PS I complexes are organized as trimers, as is evident both from electron micrographs of thylakoid membranes and from isolated PS I particles [2,3]. However, it has also been shown that the monomer–trimer equilibrium in the membrane phase should be considered as a dynamic equilibrium which can be triggered by external parameters [4,5]. Isolated trimeric complexes show an extraordinarily high density of pigment molecules in the core antenna [1]. This antenna system is relatively well separated from the redox active co-factors in the reaction center (RC) in order to be oxidation protected. The early electron transfer reactions in the RC involve six chlorophyll (Chl) molecules and two phylloquinones divided into two electron transfer branches. The six Chls of the RC are strongly coupled to each other [6–13], which leads to broadening of the covered energy spectrum and has high importance for the effective energy transfer from the different antenna compartments [14]. In addition, this interaction renders specific spectroscopic properties of the RC and hence allows its experimental observation in spectrally resolved ultrafast experiments [10,11].

Most of the known PS I complexes exhibit an intriguing feature such as the presence of the so-called 'red' Chls [15,16]. Normally, these Chls have very broad 'red'-shifted spectra. Their peculiar properties are explained by a strong excitonic interaction [17,18] and high electron–phonon coupling [18–22], likely combined with energetic shifts induced by the protein [23]. In addition, mixing with a charge transfer state was also proposed [18,20,22,24–26]. In effect the 'red' Chls absorb light with longer wavelength than the RC Chls and, even though present only in a small number, have significant influence on the energy trapping kinetics of PS I.

However, despite the increasing knowledge of the properties of these pigments, their physiological role is not clear yet. Some authors connect their role to the funnel model of the energy transfer to the RC [27], while others proposed their participation in the photoprotection [15,27–32]. Nevertheless, since the presence of the 'red' Chls do not impair the quantum efficiency of PS I their most apparent function is providing physiological advantage, through widening the spectral range of the light that can be utilized [28,33,34].

In *Thermosynechococcus elongatus* low temperature studies reveal the presence of two to three main absorption bands at 708 and 719 nm (C708 and C719) [19,21], and possibly also at 715 nm (C715) [18]. Two 'red' Chl forms are found at low temperature also in *Synechocystis* at 708 and 714 nm [20]. Currently, *Spirulina platensis* is the species with the red-most absorption bands

Abbreviations: Chl, chlorophyll; PS I, photosystem I; RC, reaction center; RP, radical pair; ET, energy transfer; CS, charge separation; DAS, decay-associated spectrum; SAES, species-associated emission spectrum; TA, transient absorption; FWHM, full width at half maximum; *S*/*N*, signal to noise ratio; DCM, 4-dicyanomethylene-2-methyl-6-p-dimethylaminostyryl-4H-pyran; β(α)-DM, n-dodecyl-β(α)-D-maltoside.

* Corresponding author. Tel.: +49 208 306 3571; fax: +49 208 306 3951.
E-mail address: holzwarth@mpi-muelheim.mpg.de (A.R. Holzwarth).
[1] Present address: Department of Biological and Geological Sciences, Faculty of Education in Al-Arish, Suez Canal University, Egypt.

0301-0104/$ - see front matter © 2009 Elsevier B.V. All rights reserved.
doi:10.1016/j.chemphys.2008.12.021

(C719 and C740) of its PS I [35]. Interestingly, a single molecule study by Brecht et al. [36] demonstrates a striking spectroscopic difference between the 'red' pools of C718 and C715/C719 in *T. elongatus*. The authors assigned the differences to the local environment and attempted to predict the position of the 'red' forms. Nonetheless, the precise location of these Chls in the core antenna system is still not identified. One of the possibilities is the monomer–monomer interaction region of the trimer [1]. Another proposed location is the vicinity of the RC in relation to a funnel model of the energy trapping [37]. In contrast, a more distant position for some or all of the 'red' pigments is suggested by other authors [20,25,38–40]. At present, few pools of Chl molecules (the trimer B31/B32/B33, and the dimers – A38/A39, A32/B7 and B37/B38) have some experimental basis [1,36] to be the most likely candidates for the formation of the so-called 'red' Chls in cyanobacteria and in particular in *T. elongatus*. However, several other Chl groups (the tetramer A31/A32/B7/B6, the trimers A2/A3/A4, A19/A20/A21 and the dimers A12/A14, A26/A27, A24/A35, A33/A34, B24/B25, B22/B34) were also proposed to contribute to the peculiar 'red' forms [23,25,41–43]. It is apparent that the uncertainty in the assignment of the 'red' pigments is fairly large, since the different proposals involve over 20% of the Chls of PS I.

In order to clarify the physiological importance of the 'red' Chls, their role in the energy trapping kinetics of PS I has to be revealed first. This will also bring more information on the position of the pigments in the complex. A number of time-resolved studies attempted to characterize the trapping kinetics. However, there is a general disagreement on the type of trapping. Based on some time-resolved fluorescence studies, Byrdin et al. suggested that the kinetics in cyanobacteria is balanced between trap- and transfer-to-trap-limited [39]. Other authors suggested a purely transfer-to-trap-limited kinetics on the basis of a non-equilibrium trapping interpretation of the time-resolved fluorescence and transient absorption data and an assumption of slow energy delivery to the RC from the antenna compartments due to the relatively large distance between them (~18 Å) [40,44–47]. A weak point in part of the latter studies is that in the analysis of the data the charge recombination reaction was not included and the possibility of de-trapping of the excitation energy from the RC was underestimated [40,44,45,47]. The charge recombination reaction, however, has been shown to play an important role in the trapping kinetics and cannot be omitted [10,48]. On the other hand, the large number of Chl molecules belonging to the antenna system of PS I, which is intimately bound to the RC, increases tremendously the de-trapping probability. The results by Savikhin et al. [46] should also be considered with care given that the authors used in their analysis the highly questionable assumption of equality of the excited state quenching processes in open and closed PS I complexes. In fact, an increase of about 12% in the fluorescence quantum yield after P700 oxidation was observed by Byrdin et al. [39], which implies a different trapping kinetics in PS I with closed RC. In contrast, a purely trap-limited kinetics is observed in some early minimal models [24,49] in cyanobacterial PS I. However, these studies lacked either sufficient time-resolution [49] or did not attempt a detailed kinetic modeling [24]. In some theoretical works [7] the trap-limited kinetics was excluded as a possibility, nevertheless, the authors discuss the relatively large probability for back energy transfer from the RC [7,26]. The problem of these models is the neglect of the charge recombination reaction, which strongly influences the result for the rate-limiting step in the calculations. Other theoretical calculations are also in favor of the transfer-to-trap-limited type of trapping kinetics [45,50]. However, in these works the authors have assumed ultrafast CS in the RC, which has no solid experimental basis [10].

The large discrepancies in all these studies originate primarily from the differences in the attempts to describe the experimental data rather than the data themselves. Generally, only a few energy transfer (ET) lifetime components are resolved. A sub-ps lifetime component describing the bulk antenna energy equilibration and one or two picosecond ET components representing the energy equilibration between the bulk antenna moiety and the 'red' Chl pools [40,51,52]. The latter components demonstrate significant non-equilibrium trapping. Finally, a 20–30 ps component is determined which is assumed to account for the main trapping [40,51,52].

A major difficulty in the spectroscopic investigation of the PS I complexes is the high pigment density, which together with the inseparability of the RC from the core antenna system, and the presence of the 'red' Chls make the experimental observation of the early electron transfer processes extremely hard. Thus the investigation of the PS I from different organisms has to be performed on the basis of the studies of the simplest possible PS I complex. Recently, such a study performed on PS I-core particles from *Chlamydomonas reinhardtii*, which do not have any 'red' Chls has brought better understanding of the trapping kinetics in PS I [10,48]. It was shown there that a charge recombination step is required for the description of the energy and charge transfer events in PS I. Furthermore, for the first time these studies resolved the excited equilibrated RC^* (i.e. excited state of the group of the six RC Chls) of PS I as a separate compartment both spectrally and kinetically. According to these results the kinetics in PS I-cores that are devoid of 'red' Chls is purely trap-limited [10].

In this work we present a time-resolved fluorescence investigation of the trapping kinetics of highly purified and intact PS I monomeric and trimeric complexes from *T. elongatus*. We demonstrate here that the energy trapping kinetics in these two complexes is identical and can be very well described with the help of the "radical pair equilibrium" model [10]. We have resolved an additional lifetime component and hence presented the existence of two separate lifetimes describing the fluorescence decay of the 'red' Chl pools. Furthermore, in accordance with our previous studies, we have estimated the rates of the primary and the secondary electron transfer reactions.

An important point for the decision on the correct trapping model is the consistency of the electron transfer reaction scheme and rates as well as the spectral properties of the RC across PS I from different species. This is important since the antenna properties and sizes vary widely for different PS I particles, while the RC properties should remain very similar. Thus only kinetic descriptions that result in the consistency of the RC properties can be considered to be adequate.

2. Materials and methods

T. elongatus was cultivated at 45 °C in a 20 L photobioreactor using BG-11 medium [53] with air enriched in 5% CO_2 [54]. Cell harvest and thylakoid membrane preparation was performed according to Rögner et al. [3] and Wenk and Kruip [55]. Monomeric and trimeric PS I complexes have been purified according to Schlodder et al. [16]. Enhancement of PS I monomers was achieved by preincubation of the thylakoid membrane in 0.6 M ammonium sulfate at 50 °C. After extraction by 0.6% n-dodecyl-β-maltoside (β-DM) and ultracentrifugation (Ti70-Rotor, 60 min, 50,000 rpm, 4 °C, Beckman), monomeric and trimeric PS I were separated by hydrophobic interaction chromatography (POROS 50-OH, Applied Biosystem, Germany) followed by ion exchange chromatography (POROS 50 HQ/M, Applied Biosystem, Germany).

The purified PS I complexes, containing 108 Chls/P700 were used for the time-resolved fluorescence measurements. The isolated monomeric and trimeric PS I particles were diluted in 30 mM HEPES buffer (pH 7.5), containing 10 mM $MgCl_2$, 10 mM

$CaCl_2$, 200 mM mannitol and 0.01% β-DM to an OD ~0.6 cm^{-1} at the Chl Q_Y maximum. The medium contained also 40 mM sodium ascorbate and 60 μM phenazine methosulfate as redox agents to keep the RCs open during the measurements.

The single-photon timing technique was used to perform picosecond time-resolved fluorescence measurements. The set-up consists of a synchronously-pumped, cavity-dumped, mode-locked dye laser at 800 kHz repetition frequency with a DCM as a laser dye [47,48]. The pulse of the dye laser has a FWHM of ~10 ps and the whole response of the system is about 30 ps FWHM, which after deconvolution results in a time-resolution of 1–2 ps. The sample was placed in a rotating cuvette (10 cm diameter, path-length of 1.5 mm) moving sideways at 66 rpm and rotating at 4200 rpm. The laser intensity at the sample was about 0.05 mW, ~0.7 mm spot diameter. Such experimental conditions ensure complete re-reduction of the RCs before the next excitation occurs. Under these conditions less than 1% of the particles receive a second laser excitation during the time they spend in the laser beam. The excitation wavelength was 663 nm to selectively excite the bulk antenna Chls. The fluorescence decays at different wavelengths were selected by a double monochromator (spectral bandwidth 4 nm). Measurements were carried out at ambient temperature (21 ± 2 °C).

Fluorescence decays were analyzed by means of global and target analyses as previously described in detail [56,57]. Global analysis is a combined mathematical fitting of the decay curves at different wavelengths done in a single fitting procedure. The analysis results in lifetimes and decay-associated spectra (DAS), describing the whole set of original data. In the more elaborate target analysis kinetic models are fitted to the data in global fashion. Such an approach leads to a physically meaningful description rate constants and spectra of the different compartments (species-associated emission spectrum (SAES)) and gives detailed information about the rate constants of the energy and electron transfer processes taking place in the investigated system. Several physically reasonable models are usually tested for their compatibility with the data.

3. Results

Time-resolved fluorescence measurements were performed on monomeric and trimeric PS I complexes from *T. elongatus* in order to investigate their light energy trapping kinetics. To avoid uncertainties in the initial energy distribution the excitation wavelength was chosen such to interact only with the pigments of the bulk antenna system (663 nm). The kinetics of the different processes in PS I was monitored by detecting the emission decays at different wavelengths from 670 to 750 nm.

3.1. Global analysis

Initially, the decays were analyzed by means of global analysis [56,57], which results in characteristic lifetimes and amplitudes (Fig. 1). For each of the two samples the minimal number of lifetime components necessary to fit the data was 5. Nevertheless, the DAS demonstrate some interesting differences. First of all, in the case of the monomeric PS I there are two lifetime components possessing the typical positive–negative amplitude feature of an ET component (3 and 9.3 ps), while the trimers have only one such component (5.5 ps). However, this 5.5 ps component has an intermediate value compared with the shortest components of the monomers and possibly represents their mixture. Secondly, the longer 20–25 and 40–50 ps components also show dissimilarities. In the monomers the ~25 ps component peaks at 720 nm and the 48 ps one – at ~730 nm, while in the trimers the corresponding components are slightly 'blue'-shifted and even show some differences in the shape of their DAS. Additionally, the amplitude ratios of the two lifetime components are different for monomers and trimers. The origin of the differences can easily be explained with some internal differences of the studied complexes. Such a preliminary conclusion, however, may be easily misleading since the global analysis is a fitting procedure with a simple sum of exponentials and does not consider some important functional relations amongst the different components. In contrast, the use of target analysis, which describes these inherent relationships correctly often, leads to resolution of lifetime components that are not fully resolved or represent mixtures in global analysis. In addition to the already described components we observe further two other longer lifetimes with small amplitude. The ns component is common for both samples and is usually encountered in all PS I studies. This lifetime is attributed to some functionally decoupled Chls. Besides that, in the trimers we observe a ~300 ps lifetime with small amplitude, whose origin is also not clear at the present moment. However, it is worth noting that the shape of its DAS is similar to the one of the longest lifetime component, which indicates that it is also related to the decoupled Chls.

In agreement with the earlier studies on cyanobacterial PS I [40,51,52], the ps lifetimes discussed above represent excitation energy equilibration between the bulk antenna Chls and the Chls from the 'red' pools. At this stage of the analysis it is not completely clear whether the ET to the 'red' Chls is not mixed with some electron transfer processes in the RC as suggested before [39,40]. So far, on the longer time scale (20–60 ps) there has only

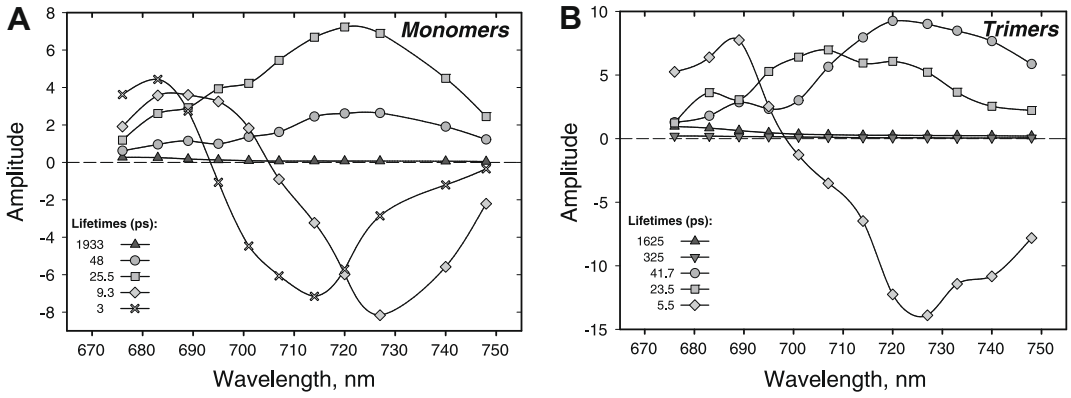

Fig. 1. Decay-associated spectra (DAS) and lifetimes of the fluorescence from monomeric (A) and trimeric (B) PS I complexes from *Thermosynechococcus elongatus* obtained through global analysis of the fluorescence decay data, λ_{exc} = 663 nm excitation. χ^2 = 1.04 and χ^2 = 1.03 for (A) and (B), respectively.

been detected one decay component [39,40,51,52], assigned as the main trapping lifetime. In our work for the first time, both in monomers and in trimers, we resolve on the longer time scale two separate lifetimes (~25 and ~45 ps). These two components possess notably 'red'-shifted DAS and in our view represent the decay kinetics of two different 'red' Chl compartments. In regard to the three 'red' pools – C708, C715 and C719, revealed by the low temperature studies of PS I from *T. elongatus* [18] one would expect to observe three lifetimes, describing the 'red' Chls kinetics. The lack of such a third lifetime component, associated with the 'red Chls' however, can be simply explained either by the kinetic and spectroscopic inseparability of two of the 'red' pools at ambient temperature or by the formation of a new 'red' state at low temperatures, which is not present otherwise.

3.2. Target analysis

The initial knowledge about the samples, obtained trough the global analysis together with the information from previous studies is used in a next step for the design of physical models. These models account for the specific features and relations between the different pigment pools in the complexes. We have tried many different kinetic models. We will however only discuss those that lead to both (i) a good fit in a mathematical sense and (ii) physically reasonable SAES. In fact the models that we found in this study could tolerate only minor changes in the rate constants (5–10%). Changes in the rate constants significantly larger than 5% bring severe deterioration of the SAES. In accordance to our earlier studies [10,48] we present here a model describing the trapping kinetics of cyanobacterial PS I monomers and trimers, which includes a fluorescing compartment representing the excited RC Chls (RC^*) (see Fig. 2). Additionally, analogous to green algae PS I [10,48] a charge recombination rate was needed to describe the time-resolved fluorescence data properly. Based on the result from the global analysis, where two separate decay components with 'red'-shifted DAS were determined in both of the investigated complexes we included in the model schemes two 'red' Chl compartments. We have also tested a model with only one 'red' state, which however did not yield physically reasonable SAES. The resulting models and the rate constants obtained after fitting to the experimental data are presented in Fig. 2. In this figure are presented also the so-called weighted eigenvector matrices, which give information for the contribution of each of the model compartments in the different decay lifetimes. In effect, by considering the physical properties of the studied complexes better resolution was achieved. The spectra of the different compartments are shown in Fig. 4.

4. Discussion

4.1. Energy transfer

The kinetic modeling of the time-resolved data demonstrates that the main part of the energy equilibration between the bulk antenna (ANT^*) and the RC (RC^*) in PS I monomers and trimers occurs on a sub-ps time scale (see Fig. 2). The different spectral properties of the model compartments together with the special kinetic relationships between them exert a constraint on the rates, which allows the estimation of lifetimes below the time-resolution of the set-up. The ratio of the corresponding forward and backward rates (~0.4) is in relatively good agreement with the one predicted by the detailed balance:

$$k_b/k_f = N_{RC}/N_{ANT} \times \exp((E_{ANT} - E_{RC})/k_B T),$$

where k_f and k_b denote the forward and backward energy transfer rates; N_{RC} and N_{ANT} the degeneracy factors for the different compartments (N_{RC} = 6, and N_{ANT} = ~90), and $k_B T$ is the Boltzmann factor. The observed ultrafast ANT^*–RC^* equilibration kinetics shows that there is no rate-limiting step in the energy delivery to the RC as proposed by others [40,44–46].The relatively high transient population of the RC^* (~13–17%) is a good argument in favor of the possibility to observe this compartment [10].

In our analysis we have also estimated the lifetimes for the energy equilibration between ANT^* and the two 'red' Chl compartments (RED^*) (Fig. 2). Apparently, for both of the 'red' compartments the process proceeds on all time scales up to ~20 ps. In agreement with previous studies [40,45,46,51] we found ~5 and ~7 ps components, which represent the main energy equilibration with the 'reds', however we observe also some additional equilibration on a later time scale for $RED1^*$. $RED1^*$ and $RED2^*$ decay correspondingly with ~44 and ~25 ps. Interestingly, the differences in the kinetics of the 'red' Chls from monomeric and trimeric complexes are only minor. A plausible explanation of this effect is that the origin of the 'red' pools is the same for both complexes, i.e. that the 'red' Chls are in fact not influenced by the trimerization. In this case, some structural changes like, e.g. detachment of Chls during previous isolation procedures can easily account for the differences with the earlier data.

In Fig. 3 is shown the population dynamics of the model compartments. The low transient population of $RED1^*$ is caused by a low ET

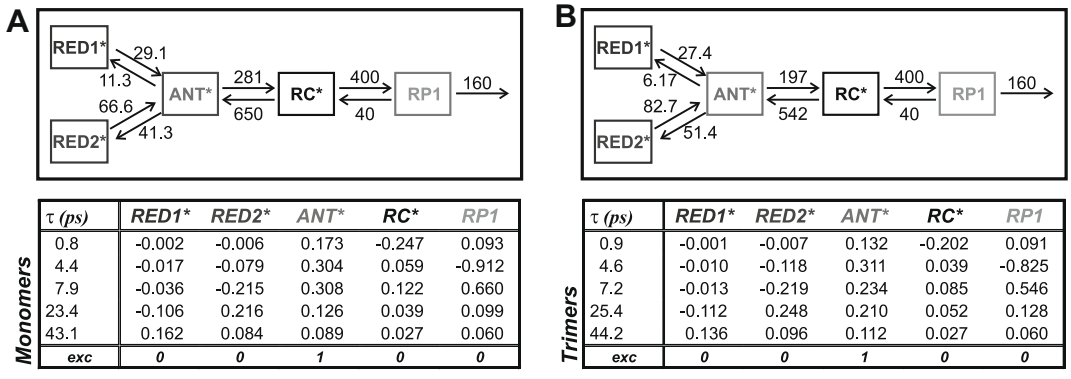

Monomers

τ (ps)	RED1*	RED2*	ANT*	RC*	RP1
0.8	-0.002	-0.006	0.173	-0.247	0.093
4.4	-0.017	-0.079	0.304	0.059	-0.912
7.9	-0.036	-0.215	0.308	0.122	0.660
23.4	-0.106	0.216	0.126	0.039	0.099
43.1	0.162	0.084	0.089	0.027	0.060
exc	0	0	1	0	0

Trimers

τ (ps)	RED1*	RED2*	ANT*	RC*	RP1
0.9	-0.001	-0.007	0.132	-0.202	0.091
4.6	-0.010	-0.118	0.311	0.039	-0.825
7.2	-0.013	-0.219	0.234	0.085	0.546
25.4	-0.112	0.248	0.210	0.052	0.128
44.2	0.136	0.096	0.112	0.027	0.060
exc	0	0	1	0	0

Fig. 2. Compartment models with rate constants (ns^{-1}) (top), lifetimes and eigenvectors (bottom) for the monomeric (A) and trimeric (B) PS I particles. χ^2 = 1.06 and χ^2 = 1.07 for (A) and (B), respectively. The errors in the rate constants are in the range of 5% and the errors in resulting lifetimes in the range of about 10%. The fastest rate constants, contributing primarily to the fastest lifetime of 0.8–0.9 ps, do have significantly larger errors (up to 15%) due to the fact that the fastest lifetime is at the resolution limit of our apparatus. Thus the fastest lifetime may have an error in the range of 20%. The advantages of global target analysis nevertheless allow resolving of these components.

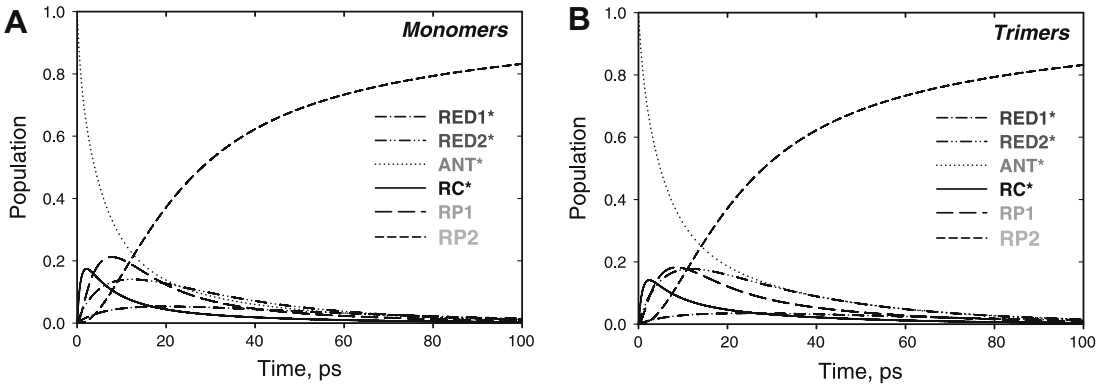

Fig. 3. Time dependence of the relative populations for the compartments from the models shown in Fig. 2. (A) PS I-monomers and (B) PS I-trimers.

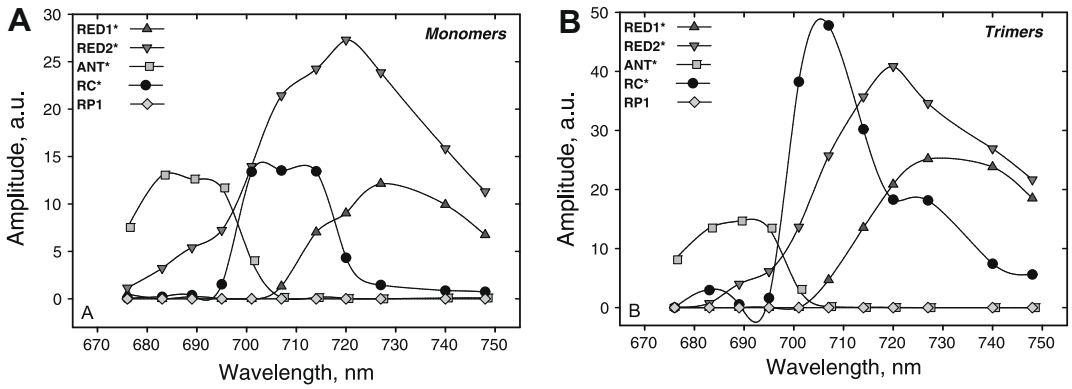

Fig. 4. Species-associated emission spectra (SAES) resulting from the modeling of the time-resolved fluorescence data of monomers (A) and trimers (B) PS I particles as shown in Fig. 2. The errors in the species-associated spectra, in particular for the RC*, compartment are directly related to the errors in the rate constants (see comment Fig. 2). Whereas the errors in the SAES for most compartments are in the range of 10%, the error for the RC* compartment could be up to 20%.

efficiency from the bulk antenna system. Such a low efficiency of this process can be explained in the light of Förster theory either by a bad spectral overlap between the compartments or by a non-favorable spatial orientation. The other 'red' compartment (RED2*), however, obtains substantial transient population (~13–17%). We performed the Boltzmann calculation also for the 'red' Chls. Unfortunately, the number of the pigments in each pool is not known, and hence the comparison with the ratio of the experimental rates is difficult. However, one can make the calculation for the forward/backward rate constants ratio using different number of Chl molecules contributing to the 'red' compartments and then do the comparison with the ratio of the rates determined from the modeling. As a result it turns out that within the given uncertainties either one or two Chl molecules can form each of the 'red' pools.

4.2. RC kinetics

One of the main elements of the presented models (Fig. 2) is the presence of a fluorescing RC* compartment. The necessity of such a compartment emerges due to the specific properties of the six RC Chls [6–13] – strong excitonic coupling, which significantly modifies the physical properties of these pigments as compared to the antenna Chls, relatively distant position from the core antenna and finally their role as electron transfer co-factors. The introduction of this compartment together with the introduction of a charge recombination rate allows the observation of the RC*, and correspondingly the initial electron transfer reactions. These features of our models are supported also by the relatively high transient population of the RC* (~13–17% in both samples) (see Fig. 3).

Within the error limits the early electron transfer reactions in the RC of both monomers and trimers occur with the same rate constants. This means that during the isolation procedures the RC of PS I is not affected, which is reasonable. The *effective CS rate* from the equilibrated RC* Chls is ~400 ns^{-1} and is similar to the one resolved in green algae (350 and 438 ns^{-1}) [10,48] and also to the one from higher plants (400 ns^{-1}) [58]. However, this rate is not the so-called *intrinsic rate of CS* from a particular electron donor pigment. The latter rate is obtained by multiplying the *effective CS rate* by the number of the pigments amongst which the RC* excitation is equilibrated, e.g. 3–6, depending on the RC exciton model. The *intrinsic rate of CS* in cyanobacterial PS I may thus vary between 1.2 and 2.4 ps^{-1} in agreement with our recent transient absorption data [10]. From the eigenvector matrix (Fig. 2) also the *apparent CS lifetime* can be obtained (**Note** that this is the main lifetime with which the first radical pair is formed, but it is **not** identical to the inverse of the above-mentioned *effective CS rate* from the RC, for detailed discussion see, e.g. [10]; the main difference is that the *apparent CS lifetime* also contains the effective antenna migration time and also reflects the statistical effects of the antenna size, i.e. in equilibrium the excited state population on the RC* is inversely proportional to the antenna size). In both of the studied PS I complexes this lifetime is ~4.5 ps, i.e. about 5–6 times shorter than the *apparent charge separation lifetime* estimated by other authors who did not resolve directly the RC* kinetics [37,40,45,46]. The free energy drop in the first electron step is ~100 meV by far larger than the one observed in PS II core complexes [59]. The decay of the first radical pair (RP1) occurs with a lifetime of ~7.5 ps. Interestingly, the secondary electron transfer reaction in cyanobacteria

seems to be accelerated in comparison to algae [48] (RP1 decay lifetime – 17 ps) and higher plants [58] (RP1 decay lifetime – 14–17 ps). This effect is in a way unexpected given that the structure of the complexes from different organisms seemed to be highly preserved. However even minor changes in the orientation of the co-factors, not resolved in the structure of higher plants [60] may bring large differences.

4.3. Fluorescence spectra of the model compartments

The target modeling of the experimental data results also in the so-called species-associated emission spectra (SAES) or simply the fluorescence spectra of each of the model compartments. In fact, SAES are one of the basic criteria for the suitability of a given model. The spectra obtained from the modeling of the data from monomers and trimers are shown in Fig. 4. The SAES of the bulk antenna (ANT^*) both in monomeric and in trimeric PS I are relatively well conserved, peaking at about 685 nm. At first glance the RC^* SAES of the two studied complexes look different; this is mainly due to two data points (707 and 727 nm), which impair the shape of the spectra. Nevertheless, the center position of the RC^* spectra is the same in monomeric and in trimeric PS I – ~705 nm. We should note here, that the SAES of the RC^* compartment is very sensitive to the determination of the shortest lifetime in the kinetics (ANT^*–RC^* energy equilibration, see Fig. 2), which in fact is at the limit of the apparatus time-resolution. In this light the difference between the RC^* SAES can be easily explained. The rest of the SAES represent the spectra of the 'red' Chl compartments. SAES of $RED2^*$ peaks at 720 nm and possesses a very broad shape, a sign for a large electron–phonon coupling, typical for the 'red' Chls [18–22]. These spectra are very well conserved in both complexes, as is the kinetics of the corresponding compartments. However, this does not apply fully for the other 'red' pool – $RED1^*$. Even though the peak wavelength and the shape remain the same, the relative intensity of this band is slightly diminished in the monomeric complexes as compared to the trimers. This effect correlates with the small differences in the kinetics. Based on the latter result we suggest that the Chls involved in the formation of the $RED2^*$ pool are not situated in close proximity to the trimerization region. However, the Chls of the $RED1^*$ pool most probably are located somewhere near this region. Nevertheless, the preserved peak position and shape of the spectra of $RED1^*$, indicates that this pool has one and the same origin in both complexes, meaning that there is no formation of a new 'red' form during the trimerization of the cyanobacterial PS I.

It is interesting to examine the changes in the DAS after analyzing the data with the help of a compartment model. These spectra for the monomeric and trimeric PS I complexes are shown in Fig. 5. As discussed above, due to the consideration of the physical relationships between the different compartments the target analysis of the data is more precise and obtains more details. This effect is apparent in the DAS after the target analysis. The ~25 ps and the ~45 ps lifetime components have better resolved DAS in contrast to the ones resulting from the global analysis (Fig. 1). In addition, higher resolution of the earlier kinetics in PS I is achieved, resolving a sub-ps component. The presence of such a lifetime component is confirmed by some transient absorption studies with higher time-resolution [24,52].

4.4. Nature of the trapping kinetics

The estimation of the rate-limiting step in the trapping kinetics is an important problem in the studies of the photosynthetic complexes, connected not only with their functionality but also with the design of artificial systems. We analyzed the results from our modeling further to gain more details about the energy trapping in cyanobacterial PS I. The average lifetime for the excited state decay in photosystems is basically the average lifetime of their fluorescence and can be presented as a sum of the lifetimes of two processes: $\tau_{avg} = \tau_{ET} + \tau_{CS}$ [58,59,61]. The first one represents the average lifetime of the energy migration in the antenna system and its delivery to the RC (τ_{ET}). In cyanobacterial PS I complexes this lifetime is influenced by the presence of the so-called 'red' Chls. The second lifetime, the average CS lifetime (τ_{CS}), accounts for the trapping of the excitations that are already located on the RC. This lifetime reveals the contribution of the CS to the total excited state decay and should not be confused with the apparent CS lifetime, which is the lifetime component describing the apparent rise of the primary RP. By scaling (multiplying by a factor both the forward and the backward rate obtained from the modeling) the ET rates ($ANT^* \leftrightarrow RC^*$) in the kinetic models (see Fig. 2) to infinity (i.e. to ensure $\tau_{ET} \ll \tau_{CS}$) the overall decay of the fluorescence will be entirely due to CS and consequently the newly calculated average lifetime will reflect exactly τ_{CS}. In this way the contributions of τ_{ET} and τ_{CS} can be calculated. The trap-limited case is realized if τ_{avg} is determined mainly by τ_{CS}, i.e. $\tau_{CS}\ \tau_{ET} > 1$. The results from this calculation are shown in Fig. 6 and Table 1. It is apparent from the ratio between the CS lifetime (τ_{CS}) and the ET lifetime (τ_{ET}) that in both monomeric and trimeric PS I-cores (2.5 and 2.04 correspondingly) the overall trapping kinetics is limited by the trap reactions, i.e. CS. Our results disagree with the theoretical modeling of Sener et al. [50] where the authors conclude that the trapping kinetics in PS I from cyanobacteria is diffusion-limited. In that work the calculated so-called first usage lifetime and the so-

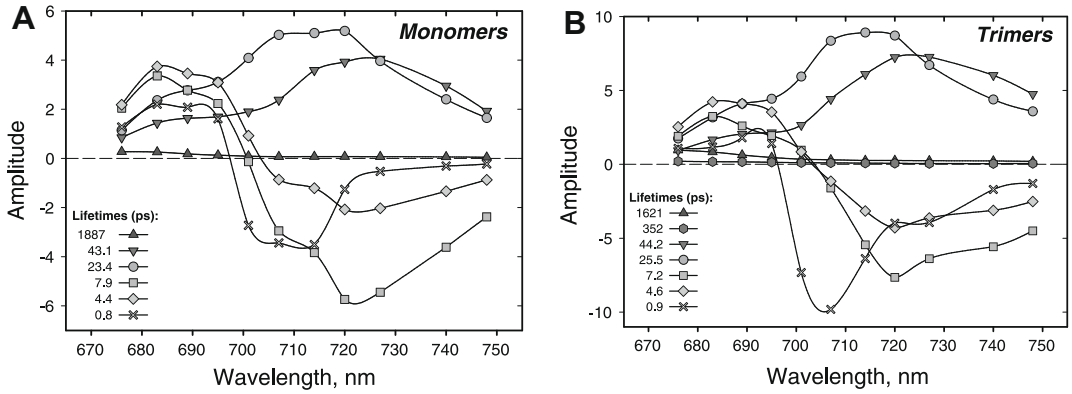

Fig. 5. DAS of PS I monomers (A) and trimers (B) recalculated from the rates and SAES of the kinetic models shown in Fig. 2. In PS I-monomers (A) the last lifetimes (~1.8 ns) and the last two (352 ps and ~1.6 ns) in trimers (B) reflect the additional components resulting from a small amount of unconnected Chls.

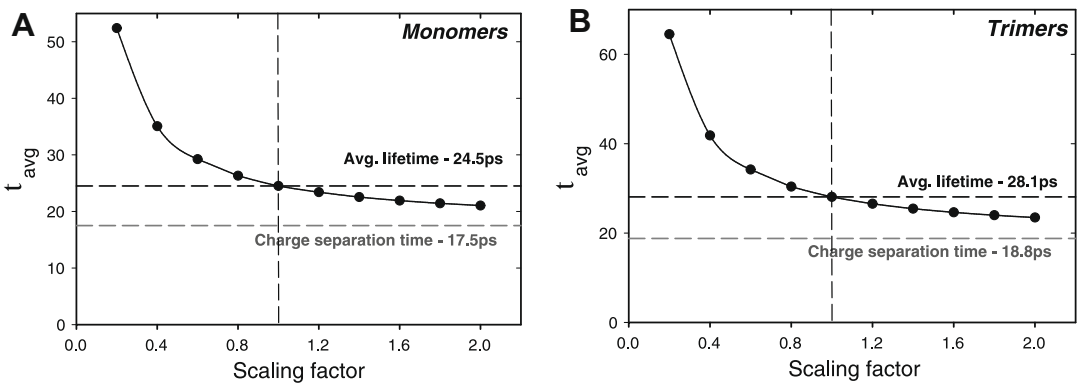

Fig. 6. Dependence of the average fluorescence lifetime (τ_{avg}) on the scaling factor of the ET rates in the kinetic models (see Fig. 2). Scaling factor 1 (vertical dashed line) corresponds to the actual situation. The scaling factor changes the ratio of the contribution of τ_{CS} and τ_{ET} to τ_{avg}. At very large scaling factors τ_{avg} approaches a limiting value (gray dashed line), which corresponds to τ_{CS}, unaffected by energy diffusion.

Table 1
Scaling analysis of the energy transfer rates (ANT*–RC* and RED*–ANT*) in the models (see Fig. 2) depending on the excitation of different compartments in the monomeric and trimeric PS I complexes. For details of the meaning of the parameters see text.

	Monomers				Trimers			
	ANT*	RED1*	RED2*	RED1/2*	ANT*	RED1*	RED2*	RED1/2*
τ_{avg} (ps)	24.5	58.3	39.4	48.8	28.1	63.9	40	52
τ_{ET} (ps)	7	33.7	14.8	24.2	9.3	35.8	11.9	23.9
τ_{CS} (ps)	17.5	24.6	24.6	24.6	18.8	28.1	28.1	28.1
τ_{CS}/τ_{ET}	2.5	0.73	1.66	1.02	2.04	0.8	2.4	1.18

journ times, which in our description correspond to τ_{ET} and τ_{CS}, bear absolutely the opposite values, even though the average lifetimes are the same (see Table 1). It seems from the latter comparison that some of the initial conditions and assumptions in their calculation were not considered properly (especially the CS rate).

4.5. Influence of the 'red' Chls on the trapping kinetics

With the help of the above-mentioned approach we performed a quantitative analysis of the impact of the 'red' Chls on the overall trapping kinetics in cyanobacterial PS I (see Tables 1 and 2). At first we scaled the forward and backward rates of the ET of the different 'red' pools (RED1*, RED2*) and then scaled also both of them together (RED1/2*), after placing the whole initial excitation into these compartments (see Tables 1 and 2). From such a calculation the type of the kinetics of the 'red' Chls becomes apparent. It is important to understand that in case that only the ET rates of the 'red pools' are scaled, the original meaning of τ_{CS} and τ_{ET} (see above) is lost to some extent. Thus, e.g. τ_{CS} will contain both ANT*–RC* energy equilibration and CS itself. However, in this case this is not a substantial disadvantage for the description since we are now interested in determining the type of the kinetics of the RED* compartments and not in determining the overall kinetics. Independent of the overall trap-limited charge separation kinetics in the whole complex, there exist a slight diffusion-limitation with regard to the energy transfer to compartment RED1*. This diffusion-limitation is however a localized effect and does not shift the trapping kinetics of the whole complex into the diffusion-limited region. The reason is that in the whole complex the overall population of compartment RED1* is relatively small (c.f. Fig. 3). The kinetics of the two 'red' compartments is very similar in monomers and in trimers (Table 1). This similarity has already been discussed (*vide supra*). However, an interesting observation is that RED1* and RED2* differ between each other in their energy transfer kinetics. While RED1* introduces a minor diffusion-limited step, the RED2* does not limit the energy transfer processes. This difference in the basic properties of the two 'red' pools are in line with the ones observed in the single molecule studies by Brecht et al. [36].

Since the 'red' Chls kinetics is now better understood it is interesting to evaluate their total effect on the kinetics and in particular on its characteristic lifetimes (τ_{avg}, τ_{ET}, τ_{CS}). Using the scaling procedures described above we calculated again the same parameters (τ_{avg}, τ_{ET}, τ_{CS}) based on the kinetic models shown in Fig. 2 but without including the 'red' compartments. This calculation provides information about the trapping kinetics in a hypothetical case where there are no 'red' Chls present. The results are shown in Table 2. Clearly the presence of the 'red' Chls introduces a deceleration of the overall trapping kinetics of ~60%. However, this overall significant effect on the total PS I kinetics not only does not impair the quantum efficiency of the complex but it also does not change the type of its kinetics.

Table 2
Effect of the 'red' Chls in PS I on the slowing down of the overall trapping kinetics. Scaling was performed as described in Table 1 and in the text. For the ANT (no REDs) case the calculation was performed without including the 'red' Chl compartments (for more details see text).

	Monomers				Trimers			
	ANT*	ANT* (No REDs)	Difference	Effect %	ANT*	ANT* (No REDs)	Difference	Effect %
τ_{avg} (ps)	24.5	13.9	10.6	56.7	28.1	16.7	11.4	68.3
τ_{ET} (ps)	7	3.6	3.4	51.4	9.3	4	5.3	43
τ_{CS} (ps)	17.5	10.3	7.2	58.8	18.8	11.7	7.1	62.2

5. Conclusions

We have described in detail the excitation energy trapping kinetics in cyanobacterial PS I monomers and trimers from *T. elongatus*. This work demonstrates the adequacy of the "charge recombination" model in the analysis of the trapping kinetics of PS I complexes. With the help of this model the RC fluorescence spectra was resolved again as in other PS I complexes, and moreover information about the early electron transfer reactions was gained. We observe an acceleration in the secondary electron transfer reaction in this thermophilic cyanobacterium in comparison to mesophiles [48,58], while the first one remains unaltered. This may well be related to the large difference in the growth temperatures these organisms are adapted to. The kinetics in both of the studied complexes was shown to be trap-limited, even though a large slowing

down effect (~60%) by the presence of the 'red' Chls was found. Our analysis revealed the presence of two separate kinetically different 'red' Chl pools both in monomers and in trimers. Some minor differences in one of the 'red' pools (RED1*) between the monomers and the trimers have been observed. However, the data strongly suggest that both of the 'red' compartments originate from the same groups of pigments in either of the two aggregation states. This precludes the location of these 'red Chl' pools immediately at the monomer–monomer interface. Thus such earlier assignments for the location of the 'red Chls' at the monomer–monomer interface, or even more extreme interpretations where the 'red' Chl pools are only created by the monomer–monomer interaction in the trimers, can be clearly excluded.

Acknowledgements

C.S. was supported by a Ph.D. Fellowship from the Max-Planck-Society. We are also grateful for the financial support from the DFG (SFB 480) and the European Union (SOLAR-H project) (to M.R.) and for a personal grant from the Egypt Government (to E. El-M.).

References

[1] P. Jordan, P. Fromme, H.T. Witt, O. Klukas, W. Saenger, N. Krauß, Nature 411 (2001) 909.
[2] E.J. Boekema, J.P. Dekker, M.G. van Heel, M. Rögner, W. Saenger, I. Witt, H.T. Witt, FEBS Lett. 217 (1987) 283.
[3] M. Rögner, U. Mühlenhoff, E.J. Boekema, H.T. Witt, Biochim. Biophys. Acta 1015 (1990) 415.
[4] D. Bald, J. Kruip, M. Rögner, Photosynth. Res. 49 (1996) 103.
[5] J. Kruip, N.V. Karapetyan, I.V. Terekhova, M. Rögner, J. Biol. Chem. 274 (1999) 18181.
[6] G.S. Beddard, Phil. Trans. Roy. Soc. Lond. A 356 (1998) 421.
[7] M. Yang, A. Damjanovic, H.M. Vaswani, G.R. Fleming, Biophys. J. 85 (2003) 140.
[8] R. Croce, G. Zucchelli, F.M. Garlaschi, R. Bassi, R.C. Jennings, Biochemistry 35 (1996) 8572.
[9] K. Gibasiewicz, V.M. Ramesh, A.N. Melkozernov, S. Lin, N.W. Woodbury, R.E. Blankenship, A.N. Webber, J. Phys. Chem. B 105 (2001) 11498.
[10] M.G. Müller, J. Niklas, W. Lubitz, A.R. Holzwarth, Biophys. J. 85 (2003) 3899.
[11] A.R. Holzwarth, M.G. Müller, J. Niklas, W. Lubitz, Biophys. J. 90 (2006) 552.
[12] K. Gibasiewicz, V.M. Ramesh, S. Lin, K. Redding, N.W. Woodbury, A.N. Webber, Biophys. J. 85 (2003) 2547.
[13] D.H. Stewart, A. Cua, D.F. Bocian, G.W. Brudvig, J. Phys. Chem. B 103 (1999) 3758.
[14] K. Gibasiewicz, V.M. Ramesh, S. Lin, N.W. Woodbury, A.N. Webber, J. Phys. Chem. B 106 (2002) 6322.
[15] N.V. Karapetyan, E. Schlodder, R. van Grondelle, J.P. Dekker, in: J.H. Golbeck (Ed.), Photosystem I: The Light-Driven, Plastocyanin: Ferredoxin Oxydoreductase, Blackwell Publishers, 2006, p. 177.
[16] E. Schlodder, V.V. Shubin, E. El-Mohsnawy, M. Roegner, N.V. Karapetyan, Biochim. Biophys. Acta 1767 (2007) 732.
[17] B. Gobets, H. van Amerongen, R. Monshouwer, J. Kruip, M. Rögner, R. van Grondelle, J.P. Dekker, Biochim. Biophys. Acta 1188 (1994) 75.
[18] V. Zazubovich, S. Matsuzaki, T.W. Johnson, J.M. Hayes, P.R. Chitnis, G.J. Small, Chem. Phys. 275 (2002) 47.
[19] L.-O. Palsson, J.P. Dekker, E. Schlodder, R. Monshouwer, R. van Grondelle, Photosynth. Res. 48 (1996) 239.
[20] M. Rätsep, T.W. Johnson, P.R. Chitnis, G.J. Small, J. Phys. Chem. B 104 (2000) 836.
[21] F. Jelezko, C. Tietz, U. Gerken, J. Wrachtrup, R. Bittl, J. Phys. Chem. B 104 (2000) 8093.
[22] J.A. Ihalainen, M. Rätsep, P.E. Jensen, H.V. Scheller, R. Croce, R. Bassi, J.E.I. Korppi-Tommola, A. Freiberg, J. Phys. Chem. B 107 (2003) 9086.
[23] A. Damjanovic, H. Vaswani, P. Fromme, G.R. Fleming, J. Phys. Chem. B 106 (2002) 10251.
[24] A.N. Melkozernov, S. Lin, R.E. Blankenship, Biochemistry 39 (2000) 1489.
[25] S. Vaitekonis, G. Trinkunas, L. Valkunas, Photosynth. Res. 86 (2005) 185.
[26] H.M. Vaswani, J. Stenger, P. Fromme, G.R. Fleming, J. Phys. Chem. B 110 (2006) 26303.
[27] A.N. Melkozernov, R.E. Blankenship, Photosynth. Res. 85 (2005) 33.
[28] N.V. Karapetyan, A.R. Holzwarth, M. Rögner, FEBS Lett. 460 (1999) 395.
[29] N.V. Karapetyan, Biophysics 49 (2004) 196.
[30] D. Carbonera, G. Agostini, T. Morosinotto, R. Bassi, Biochemistry 44 (2005) 8337.
[31] A.F. Elli, F. Jelezko, C. Tietz, H. Studier, M. Brecht, R. Bittl, J. Wrachtrup, Biochemistry 45 (2006) 1454.
[32] R. Croce, M. Mozzo, T. Morosinotto, A. Romeo, R. Hienerwadel, R. Bassi, Biochemistry 46 (2007) 3846.
[33] H.-W. Trissl, Photosynth. Res. 35 (1993) 247.
[34] A. Rivadossi, G. Zucchelli, F.M. Garlaschi, R.C. Jennings, Photosynth. Res. 60 (1999) 209.
[35] N.V. Karapetyan, V.V. Shubin, S.S. Vasiliev, I.N. Bezsmertnaya, V.B. Tusov, V.Z. Pashchenko, in: N. Murata (Ed.), Research in Photosynthesis, Kluwer, Dordrecht, 1992, p. 549.
[36] M. Brecht, H. Studier, A.F. Elli, F. Jelezko, R. Bittl, Biochemistry 46 (2007) 799.
[37] A.N. Melkozernov, S. Lin, R.E. Blankenship, J. Phys. Chem. B 104 (2000) 1651.
[38] L.-O. Palsson, C. Flemming, B. Gobets, R. van Grondelle, J.P. Dekker, E. Schlodder, Biophys. J. 74 (1998) 2611.
[39] M. Byrdin, I. Rimke, E. Schlodder, D. Stehlik, T.A. Roelofs, Biophys. J. 79 (2000) 992.
[40] B. Gobets, I.H.M. van Stokkum, M. Rögner, J. Kruip, E. Schlodder, N.V. Karapetyan, J.P. Dekker, R. van Grondelle, Biophys. J. 81 (2001) 407.
[41] M. Byrdin, P. Jordan, N. Krauss, P. Fromme, D. Stehlik, E. Schlodder, Biophys. J. 83 (2002) 433.
[42] P. Fromme, P. Jordan, N. Krauß, Biochim. Biophys. Acta 1507 (2001) 5.
[43] M.K. Sener, D.Y. Lu, T. Ritz, S. Park, P. Fromme, K. Schulten, J. Phys. Chem. B 106 (2002) 7948.
[44] B. Gobets, R. van Grondelle, Biochim. Biophys. Acta 1507 (2001) 80.
[45] B. Gobets, I.H.M. van Stokkum, F. van Mourik, J.P. Dekker, R. van Grondelle, Biophys. J. 85 (2003) 3883.
[46] S. Savikhin, W. Xu, P. Martinsson, P.R. Chitnis, W.S. Struve, Biochemistry 40 (2001) 9282.
[47] R. Croce, D. Dorra, A.R. Holzwarth, R.C. Jennings, Biochemistry 39 (2000) 6341.
[48] A.R. Holzwarth, M.G. Müller, J. Niklas, W. Lubitz, J. Phys. Chem. B 109 (2005) 5903.
[49] A.R. Holzwarth, G.H. Schatz, H. Brock, E. Bittersmann, Biophys. J. 64 (1993) 1813.
[50] M.K. Sener, S. Park, D.Y. Lu, A. Damjanovic, T. Ritz, P. Fromme, K. Schulten, J. Chem. Phys. 120 (2004) 11183.
[51] A.N. Melkozernov, V.H.R. Schmid, S. Lin, H. Paulsen, R.E. Blankenship, J. Phys. Chem. B 106 (2002) 4313.
[52] S. Savikhin, W. Xu, V. Soukoulis, P.R. Chitnis, W.S. Struve, Biophys. J. 76 (1999) 3278.
[53] R. Rippka, J. Deruelles, J.B. Waterbury, M. Herdman, R.Y. Stanier, J. Gen. Microbiol. 111 (1979) 1.
[54] H. Kuhl, J. Kruip, A. Seidler, A. Krieger-Liszkay, M. Bunker, D. Bald, A.J. Scheidig, M. Rögner, J. Biol. Chem. 275 (2000) 20652.
[55] S.-O. Wenk, J. Kruip, J. Chromatogr. B 737 (2000) 131.
[56] A.R. Holzwarth, in: J. Amesz, A.J. Hoff (Eds.), Biophysical Techniques in Photosynthesis. Advances in Photosynthesis Research, Kluwer Academic Publishers, Dordrecht, 1996, p. 75.
[57] I.H.M. van Stokkum, D.S. Larsen, R. van Grondelle, Biochim. Biophys. Acta 1657 (2004) 82.
[58] C. Slavov, M. Ballottari, T. Morosinotti, R. Bassi, A.R. Holzwarth, Biophys. J. 94 (2008) 3601.
[59] Y. Miloslavina, M. Szczepaniak, M.G. Müller, J. Sander, M. Nowaczyk, M. Rögner, A.R. Holzwarth, Biochemistry 45 (2006) 2436.
[60] A. Amunts, O. Drory, N. Nelson, Nature 447 (2007) 58.
[61] R. van Grondelle, B. Gobets, in: G.C. Papageorgiou, Govindjee (Eds.), Chlorophyll a Fluorescence. A Signature of Photosynthesis, Springer, Dordrecht, 2004, p. 107.